Interaction with host SGS3 is required for suppression of RNA silencing by tomato yellow leaf curl virus V2 protein

Efrat Glick*, Avi Zrachya*, Yael Levy*, Anahit Mett*, David Gidoni*, Eduard Belausov*, Vitaly Citovsky†, and Yedidya Gafni*‡

*Institute of Plant Sciences, Agricultural Research Organization, Volcani Center, P. O. Box 6, Bet Dagan 50250, Israel; and †Department of Biochemistry and Cell Biology, State University of New York, Stony Brook, NY 11794-5215

Edited by Deborah P. Delmer, University of California, Davis, CA, and approved November 15, 2007 (received for review September 23, 2007)

The V2 protein of tomato yellow leaf curl geminivirus (TYLCV) functions as an RNA-silencing suppressor that counteracts the innate immune response of the host plant. The host-cell target of V2, however, remains unknown. Here we show that V2 interacts directly with SlSGS3, the tomato homolog of the *Arabidopsis* SGS3 protein (AtSGS3), which is known to be involved in the RNA-silencing pathway. *SlSGS3* genetically complemented an *AtSGS3* mutation and restored RNA silencing, indicating that SlSGS3 is indeed a functional homolog of AtSGS3. A point mutant of V2 that is unable to bind SlSGS3 also lost its ability to suppress RNA silencing, suggesting a correlation between the V2–SlSGS3 interaction *in planta* and the suppressor activity of V2.

Plants have evolved an innate immune response to invading viruses that is based on posttranscriptional RNA silencing (1–4). RNA silencing induced by transcripts of sense transgenes and viral DNA genomes is thought to involve conversion of single-stranded (ss) RNA species into double-stranded (ds) RNA by RDR6, with the help of SGS3 (5–7). Alternatively, SGS3 may be involved in the transport of the RNA-silencing signal (8). dsRNAs are processed by the cellular machinery to produce siRNAs that are incorporated into RNA-induced silencing complexes (RISCs), within which siRNAs direct the cleavage of the complementary viral transcripts (9, 10).

To counteract the plant antiviral response, many viruses produce suppressor proteins that block the host RNA silencing by targeting different steps of the silencing pathway (11–14). For example, the potyviral HcPro most likely inhibits unwinding of the siRNA duplex and RISC assembly (10), P25 of *Potato virus X* suppresses the production or accumulation of mobile silencing signals (15), and P19 of *Tomato bushy stunt virus* (TBSV) and P21 of *Beet yellow virus* inhibit RNA silencing by physically interacting with siRNAs and preventing their processing or incorporation into the RISC (9, 10, 16–20). However, among numerous known viral RNA-silencing suppressors, only two, the 2b protein of *Cucumber mosaic virus* (CMV) and poleroviral (P0), have been shown to interact directly with a protein component of the host-silencing pathway. Specifically, CMV 2b binds AGO1 and inhibits its endonucleolytic activity (21), and P0 targets AGO1 for degradation (22). Here we report that an RNA-silencing suppressor of *Tomato yellow curl leaf geminivirus* (TYLCV), the V2 protein (23), interacts directly with the host SGS3 *in planta*, and that this interaction is required for V2's ability to suppress RNA silencing.

Results

V2 Interacts with Tomato and *Arabidopsis* SGS3. To identify a host-cell target of V2, we used a two-hybrid screen (24, 25) with a tomato (*Solanum lycopersicum*) cDNA library and the V2 protein as bait. Screening of $\approx 1 \times 10^6$ transformants resulted in the identification and isolation of four independent cDNA clones producing V2 interactors, two of which represented the same cDNA clone. Coexpression of V2 and one of its interactors, designated SlSGS3 (GenBank accession no. EF590136), activated the *LEU2* reporter gene and enabled yeast transformants to grow on a leucine dropout medium. This interaction was specific because the cells that were cotransformed with either the V2-expressing construct and the empty library vector pJG4-5, or with the SlSGS3-expressing construct and pEG202-expressing Bicoid homeodomain (pRFHM1), which is often used to detect nonspecific two-hybrid interactions (26), were unable to survive in the absence of leucine (Fig. 1*A*). Cells expressing all three combinations of proteins grew to the same extent in the presence of leucine (data not shown), indicating that the tested proteins did not adversely and nonspecifically affect yeast-cell physiology. Amino acid sequence analysis revealed significant homology between the identified V2 interactor, SlSGS3, and *Arabidopsis* SGS3 (AtSGS3) (Fig. 1*B*). As is typical for members of the SGS3 protein family (27), both SlSGS3 and AtSGS3 contained a conserved XS domain with an as-yet-unknown function (Fig. 1*B*) (27).

Next, we examined the subcellular localization patterns of YFP-tagged SlSGS3 or AtSGS3 coexpressed with CFP-tagged V2. Fig. 2 shows that, in tobacco protoplasts, V2-CFP coexpressed with YFP-SlSGS3 (Fig. 2*A*) or YFP-AtSGS3 (Fig. 2*B*) accumulates in distinct microbodies throughout the cell cytoplasm, and that the accumulated SlSGS3 or AtSGS3 largely colocalizes with V2. These observations were confirmed in leaf tissues of tomato, the native TYLCV host (Fig. 2*C*). SlSGS3/V2 colocalization was then quantified by counting the corresponding microbodies that overlapped within the coexpressing cell. These calculations showed that, on average, 97% of V2 colocalized with SlSGS3 and 86% of SlSGS3 colocalized with V2, suggesting that most of these protein microbodies overlap within the coexpressing cells. This colocalization of SlSGS3/AtSGS3 and V2 is consistent with their ability to interact with one another.

Interestingly, the colocalization experiments also suggested that neither V2 nor SlSGS3 can move between plant cells. Because agroinfiltration is performed with a mixture of two bacterial strains, each carrying one of the tested genes, the target cells are sometimes transformed by only one bacterial strain, resulting in cells that express a single tagged protein (i.e., either V2 or SGS3). This finding is exemplified in Fig. 2*C*, which shows two adjacent cells (1 and 2). Cell 1 expressed both SlSGS3 and V2, and cell 2 expressed only SlSGS3. Fig. 2*D* shows the reciprocal situation, with cell 1 expressing both SlSGS3 and V2

Author contributions: V.C. and Y.G. designed research; E.G., A.Z., Y.L., A.M., and E.B. performed research; E.G. and D.G. analyzed data; and V.C. and Y.G. wrote the paper.

The authors declare no conflict of interest.

This article is a PNAS Direct Submission.

Data deposition: The sequences reported in this paper have been deposited in the GenBank database (accession nos. EF590136 and AF234296).

‡To whom correspondence should be addressed. E-mail: ygafni@volcani.agri.gov.il.

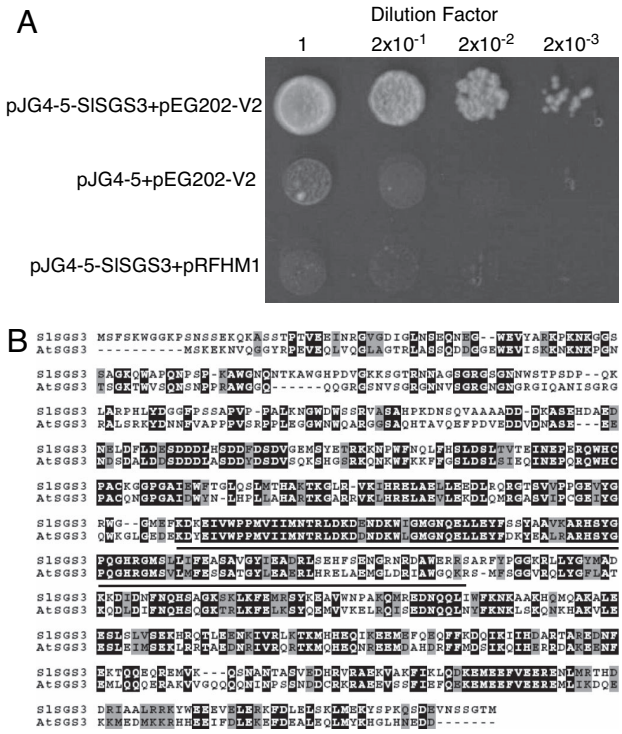

Fig. 1. Identification of SlSGS3 and its interaction with TYLCV V2 in yeast. (*A*) Interaction in yeast two-hybrid system. The indicated cell inocula were plated on growth media without leucine, tryptophan, histidine, or uracil. Because growth on leucine-deficient medium represents selective conditions for protein–protein interactions, efficient growth of cells coexpressing SlSGS3 and V2 indicated interaction between these proteins, whereas the absence of cell growth in two negative controls indicated the specificity of this interaction. (*B*) Alignment of the SlSGS3 with AtSGS3. Regions of identity and similarity are indicated by black and shaded boxes, respectively; gaps introduced for alignment are indicated by dashes. The XS domain is denoted by a horizontal bar under its sequence. Alignment was performed by using the ClustalW algorithm (www.genebee.msu.su/clustal/advanced.html).

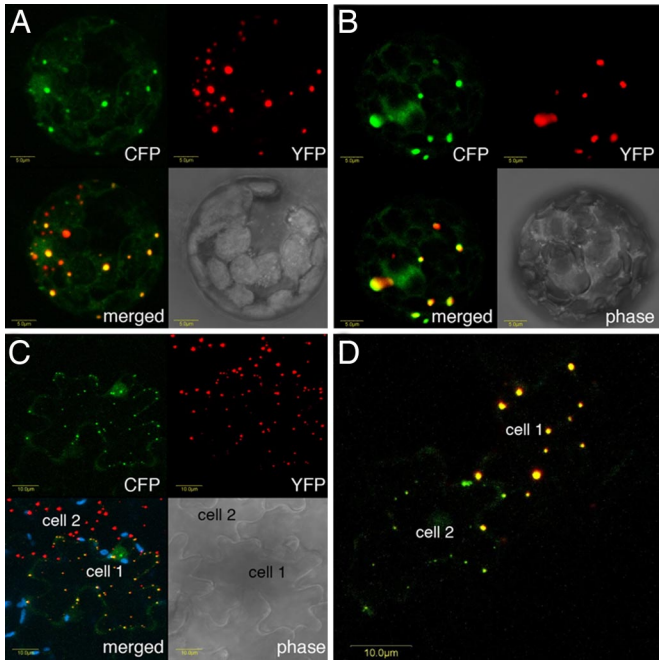

Fig. 2. Subcellular colocalization of V2 with SlSGS3 and AtSGS3. (*A* and *B*) V2-CFP coexpressed with YFP-SlSGS3 or YFP-AtSGS3, respectively, in *N. tabacum* protoplasts. (*C* and *D*) V2-CFP coexpressed with YFP-SlSGS3 in agroinfiltrated tomato leaf epidermis. Note that, adjacent to the coexpressing cell (cell 1), *C* and *D* also show a cell (cell 2) that expresses either YFP-AtSGS3 or V2-CFP, respectively. CFP signal is shown in green, YFP signal is shown in red, and signal produced by comparable levels of the colocalizing proteins is shown in yellow. Plastid autofluorescence was filtered out in *A* and *B* and is shown in blue in *C*. All images are projections of several confocal sections.

and cell 2 expressing only V2. These data suggest that there is no transport of V2 or SlSGS3 from the expressing cell to the adjacent cell that does not express these proteins.

The interaction of V2 with SlSGS3 and AtSGS3 was demonstrated directly *in planta* by FRET microscopy, which allows for the detection of protein interactions within living cells, as well as a determination of the subcellular localization of the interacting proteins (28, 29). YFP-SlSGS3 or YFP-AtSGS3 was transiently coexpressed with V2-CFP in tobacco protoplasts. FRET between these proteins was detected by acceptor photobleaching (30, 31). Fig. 3 indicates colocalization and energy transfer between YFP-SlSGS3 and V2-CFP and between YFP-AtSGS3 and V2-CFP at punctate locations in the cell cytoplasm.

Quantification of the CFP signal after photobleaching of YFP revealed an increase in the intensity of the donor fluorescence with a FRET efficiency (E_F) of 32.2 ± 8.0% and 32.6 ± 5% for YFP-SlSGS3/V2-CFP and YFP-AtSGS3/V2-CFP, respectively, which is indicative of FRET (30, 31). As expected, free coexpressed YFP and CFP did not generate detectable FRET (Fig. 3*C*).

SlSGS3 Functionally Complements an *Arabidopsis* sgs3 Mutant. To directly demonstrate that SlSGS3 in fact represents a functional SGS3 protein, we examined whether the *SlSGS3* gene can complement the known RNA-silencing-deficient phenotype of the L1/sgs3-1 *Arabidopsis* line (8), in which a chemically induced *sgs3-1* mutation of *AtSGS3* abrogates RNA silencing of a tandem arrangement of the β-glucuronidase (GUS) transgene in the parental L1 transgenic line (32). We produced double-transgenic plants that constitutively expressed the *SlSGS3* cDNA (L1/sgs3-1/SlSGS3) or *AtSGS3* cDNA (L1/sgs3-1/AtSGS3). The resultant plants were first examined for the presence and expression of the *SlSGS3* or *AtSGS3* transgenes. PCR-based analysis by using *SlSGS3*- and *AtSGS3*-specific primers revealed the presence of the *SlSGS3* sequences in L1/sgs3-1/SlSGS3, but not in L1/sgs3-1 parental control plants (Fig. 4*A*). Both L1/sgs3-1/AtSGS3 and L1/sgs3-1 plants contained the endogenous *AtSGS3* gene, distinguished by its larger size because of the presence of the intron, but only L1/sgs3-1/AtSGS3 contained the AtSGS3 cDNA transgene (Fig. 4*A*). Our RT-PCR analysis by using primers specific for the *SlSGS3* and *AtSGS3* transgenes, but not for the endogenous *AtSGS3* gene, detected the corresponding transcripts only in L1/sgs3-1/SlSGS3 and L1/sgs3-1/AtSGS3 plants, respectively. In control experiments, analysis of actin-specific transcripts generated similar amounts of PCR products in all samples, indicating equal efficiencies of the RT-PCRs (Fig. 4*B*).

Next, four independent lines of L1/sgs3-1/SlSGS3 and 10 independent lines of L1/sgs3-1/AtSGS3, as well as the parental plants L1/sgs3-1 and L1, were examined for their ability to silence the GUS reporter transgene. Fig. 4*C* shows that, although the L1/sgs3-1 plants exhibited significant levels of GUS expression, both L1/sgs3-1/SlSGS3 and L1/sgs3-1/AtSGS3 plants efficiently silenced the transgene. This silencing was comparable to that observed in the original L1 silenced line (Fig. 4*C*). These observations indicate that the *SlSGS3* cDNA genetically complements the *sgs3-1* mutation, suggesting that SlSGS3 represents a functional homolog of AtSGS3.

The V2–SlSGS3 Interaction Is Required for RNA Silencing. To correlate between V2–SlSGS3 binding and the RNA-silencing-suppressor

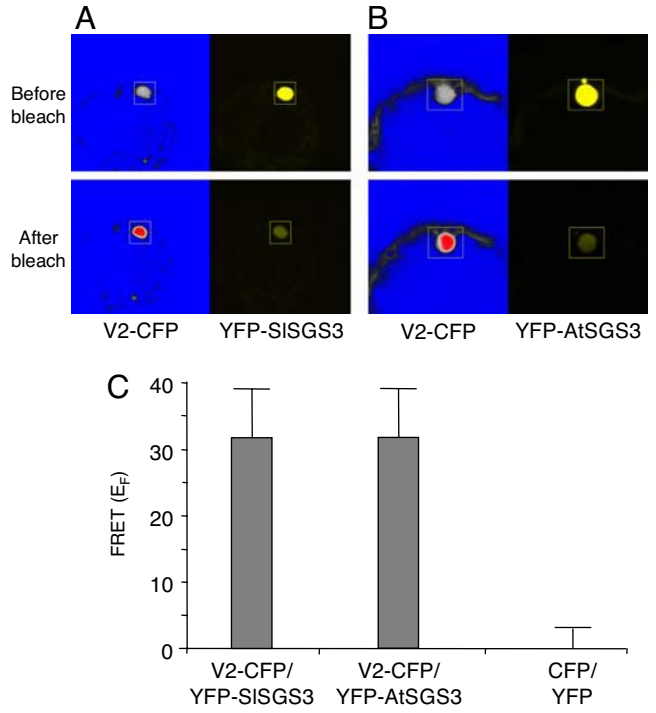

Fig. 3. Interaction between V2 and SlSGS3 or AtSGS3 *in planta*. (*A* and *B*) Protein–protein interaction was monitored by FRET microscopy of living *N. tabacum* protoplasts coexpressing V2-CFP and either YFP-SlSGS3 (*A*) or YFP-AtSGS3 (*B*). Representative acceptor photobleaching images show CFP (donor) and YFP (acceptor) channels before and after bleaching. After bleaching, CFP fluorescence increases and YFP fluorescence decreases in the bleached areas indicated by rectangles. All images are projections of several confocal sections. (*C*) Quantification of donor fluorescent intensity in representative samples. Data represent average values of three independent experiments, with 10 protoplasts each, with indicated standard deviation values.

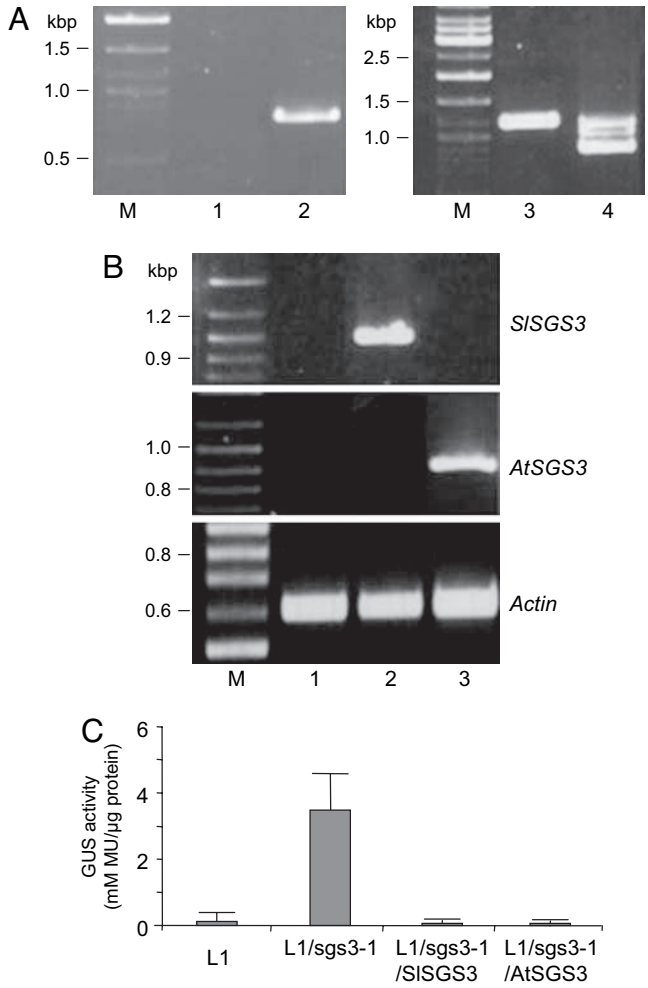

Fig. 4. Genetic complementation of the *Arabidopsis L1/sgs3-1* phenotype by *SlSGS3* and restoration of RNA silencing. (*A*) PCR-based identification of L1/sgs3-1/SlSGS3 and L1/sgs3-1/AtSGS3 transgenic plants by detection of the *SlSGS3* (*Left*) and *AtSGS3* (*Right*) transgenes, respectively. Lane M, molecular size markers [indicated in kilobase pairs (kbp)]; lane 1, L1/sgs3-1 parental line showing no *SlSGS3* cDNA-specific PCR product; lane 2, L1/sgs3-1/SlSGS3 line producing the *SlSGS3* cDNA-specific 786-bp PCR product; lane 3, L1/sgs3-1 parental line showing a 1,191-bp PCR product specific for the endogenous *AtSGS3* gene with its intron, but no AtSGS3 cDNA-specific 888-bp band; lane 4, L1/sgs3-1/AtSGS3 plants yielding 1,191- and 888-bp PCR products specific for the intron-containing endogenous *AtSGS3* gene and the *AtSGS3* cDNA transgene, respectively. (*B*) RT-PCR-based detection of transcripts derived from the *SlSGS3* and *AtSGS3* cDNA transgenes. Lane M, molecular size markers (kbp); lane 1, L1/sgs3-1 parental line; lane 2, L1/sgs3-1/SlSGS3 plants; lane 3, L1/sgs3-1/AtSGS3 plants. L1/sgs3-1/SlSGS3 and L1/sgs3-1/AtSGS3 plants yielded RT-PCR products specific for the *SlSGS3* and *AtSGS3* transcripts, respectively, whereas all plants contained transcripts of the constitutively expressed *Actin* gene. (*C*) Silencing of the GUS reporter in the indicated plant lines. Note that expression of *SlSGS3* or *AtSGS3* transgenes restored RNA silencing of *GUS* in L1/sgs3-1 plants to levels comparable to those of the original silenced L1 line. Data represent average values of three independent experiments with indicated standard deviations.

activity of V2, we used a substitution mutant of V2, C84S/C86S. First, consistent with previous observations (23), we showed that the C84S/C86S mutant was indeed compromised in its ability to suppress RNA silencing. RNA silencing was detected by a visible increase in GFP expression after coinfiltration of a wild-type *Nicotiana benthamiana* plant with two strains of *Agrobacterium*, one that carries V2 or its mutant and the other that contains the RNA-silencing initiator and reporter gene, GFP (23). *GFP* expression, which could be observed 2 days postinfiltration (dpi) (data not shown), was almost completely silenced at 7 dpi. This silencing was efficiently suppressed by the coexpressed V2, resulting in easily detectable GFP fluorescence (Fig. 5*A*). The C84S/C86S mutant of V2 lost its RNA-silencing-suppression activity, failing to restore GFP expression in the inoculated leaves (Fig. 5*A*). These results were confirmed by RT-PCR analyses of *GFP* transcripts (data not shown).

We then examined the effects of the C84S/C86S mutation on V2's subcellular localization and interaction with SlSGS3. Fig. 5*B* shows that the C84S/C86S mutant exhibited the same microbody-associated localization pattern as the wild-type V2 (compare with Fig. 2*A*), indicating that the mutation did not significantly alter the subcellular distribution of the protein. The FRET studies, however, showed that the mutant V2 lost most of its ability to interact with SlSGS3 (Fig. 5*C*). These results suggest that disrupting the V2–SlSGS3 interaction substantially impairs the suppressor function of V2, but does not interfere with the overall accumulation and subcellular distribution of the protein, effectively uncoupling between colocalization and protein–protein interaction.

Discussion

TYLCV is a member of the Geminiviridae family of plant viruses characterized by their ssDNA genome, which replicates and transcribes in the host-cell nucleus. Although TYLCV is a DNA virus that replicates by a dsDNA intermediate, it is capable of inducing RNA silencing in infected plants (33, 34). This antiviral reaction is counteracted by RNA-silencing suppressors encoded by several geminiviruses (14), as well as by many other plant

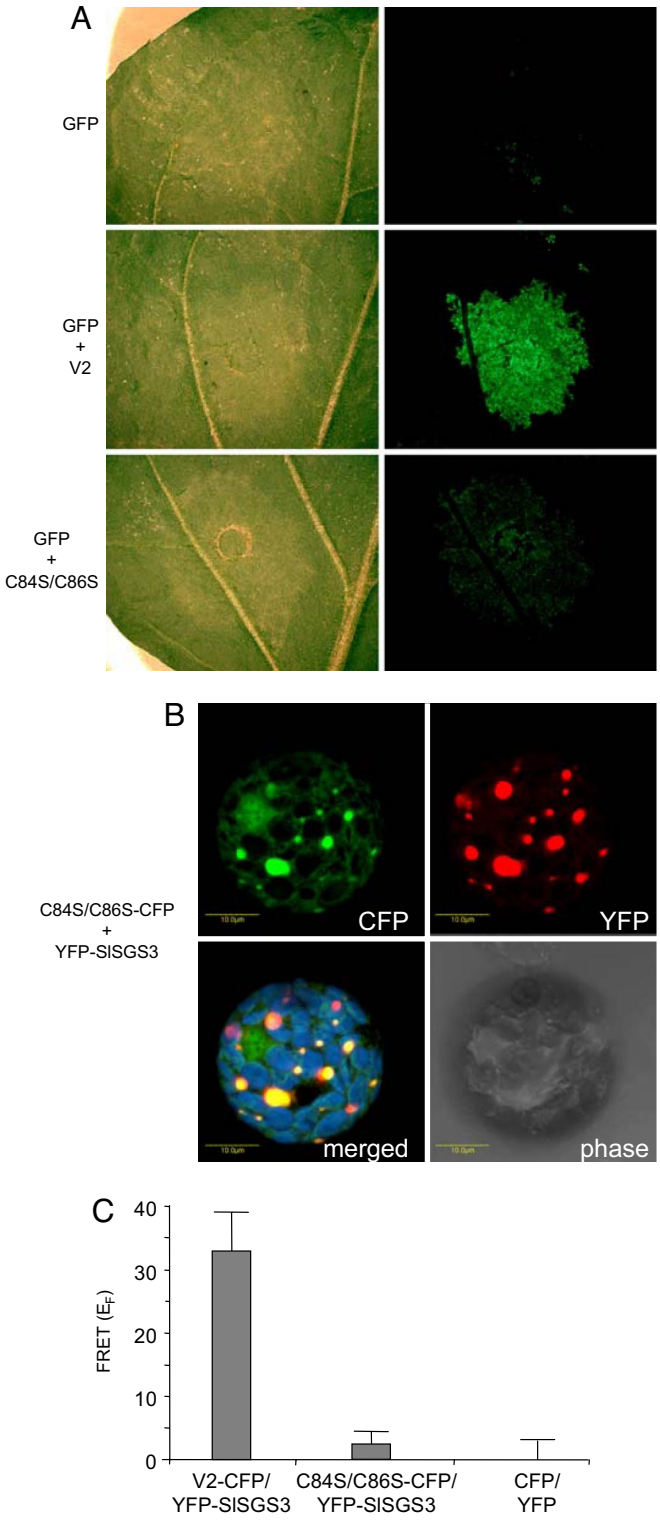

Fig. 5. Correlation between V2-induced suppression of RNA silencing and V2-SlSGS3 binding. V2 and its C84S/C86S mutants were tested for their ability to suppress RNA silencing, subcellular localization, and interaction with SlSGS3. (*A*) RNA-silencing suppression. *N. benthamiana* leaves were agroinfiltrated with a mixture of a GFP-expressing construct and an empty expression vector (GFP), a V2-expressing vector (GFP+V2), or a C84S/C86S-expressing vector (GFP+C84S/C86S). (*Left*) Leaves 7 days after infiltration. (*Right*) GFP fluorescence in the same leaves. (*B*) Subcellular localization in *N. tabacum* protoplasts coexpressing C84S/C86S-CFP and YFP-SlSGS3. CFP signal is shown in green, YFP signal is shown in red, comparable levels of colocalizing green and red signals produce yellow color, and plastid autofluorescence is shown in blue. Images are projections of several confocal sections. (*C*) Interaction with SlSGS3. By using FRET microscopy, donor fluorescent intensity was quantified in representative samples. Data represent average values of three independent experiments, with 10 protoplasts each, with indicated standard deviation values.

viruses (11–13). Of these viral proteins, TYLCV V2 is only the second reported RNA-silencing suppressor, after CMV 2b (21), that is likely to target a protein component of the host RNA-silencing machinery directly. Unlike 2b, however, which interacts with the AGO1 endonuclease component of the RISC (21), V2 binds SGS3, whose function in the silencing pathway remains unclear, but may include production of dsRNA (5), transport of the RNA-silencing signal (8), or protection of transcript fragments from degradation, allowing RDR6 to generate duplex RNA (35).

Because TYLCV is a geminivirus, it is especially interesting that SGS3 is specifically required for the RNA-silencing defense against geminiviruses (6). Thus, interaction of V2 with SGS3 makes biological sense. We suggest that V2 binding may inactivate SGS3, thereby blocking the silencing pathway. Because SGS3 most likely performs a stoichiometric, rather than an enzymatic, function (5, 8, 35), binding to and potentially disabling a large proportion of cellular SGS3 by V2 produced by the invading virus would substantially impair SGS3's function during RNA silencing. This finding is consistent with our observations that the overexpression of V2 from a strong 35S promoter in cells that express the *SGS3* gene from the weaker native promoter results in strong suppression most likely because of more efficient binding of SGS3 by the excess amounts of V2. Furthermore, the fact that the V2 mutant, which is unable to bind SGS3, loses its ability to suppress silencing supports our notion that the V2–SGS3 interaction may represent one of the key events in V2-induced RNA-silencing suppression in TYLCV-infected plant cells.

Potential inactivation of SGS3 by V2 also may affect the development of TYLCV disease symptoms. TYLCV-infected tomatoes are distinguished by curling of their leaves (36), and tomato plants carrying a mutation within the *SGS3* locus exhibit an aberrant leaf phenotype (Y. Eshed, personal communication). Consistent with this effect on leaf morphology, SGS3 also has been implicated in determining the adaxial identity of the leaf (37). Besides helping to better understand the complex nature of the TYLCV–host interaction, our observations may be useful in designing new approaches to combating viral infection, for example, by disrupting the V2–SGS3 interaction.

Materials and Methods

Plasmid Construction. To produce a bait construct, the PCR-amplified ORF of TYLCV V2 (23) was inserted into the EcoRI-XhoI sites of pEG202 (38), resulting in pEG202-V2.

For subcellular localization studies, TYLCV-Is V2 was tagged at its C terminus with CFP by cloning a PCR-amplified V2 ORF into the BglII-EcoRI sites of pSAT6A-ECFP-N1 (39), resulting in pSAT6A-V2-ECFP. Then the expression cassette of pSAT6A-V2-ECFP was PCR-amplified and inserted into the HindIII-SacI sites of pCAMBIA1300 (GenBank accession no. AF234296), resulting in pCAMBIA1300-V2-CFP. SlSGS3 and AtSGS3 were tagged at their N termini with YFP by cloning PCR-amplified *SlSGS3* or *AtSGS3* cDNAs into the EcoRI-BamHI or XhoI-BamHI sites, respectively, of pSAT6-EYFP-C1 (39), resulting in pSAT6-EYFP-SlSGS3 and pSAT6-EYFP-AtSGS3, respectively. The expression cassette from pSAT6-EYFP-SlSGS3 was then PCR-amplified and inserted into the SalI-KpnI sites of pCAMBIA1300, resulting in pCAMBIA1300-EYFP-SlSGS3.

For genetic complementation studies, the *SlSGS3* or *AtSGS3* cDNAs were first cloned into the XhoI-BamHI sites of pSAT6A-MCS (39), and then the constitutive expression cassettes were PCR-amplified and inserted into the SalI-EcoRI or SalI-SacI sites, respectively, of pCAMBIA1300 to produce pCAMBIA1300-SlSGS3 and pCAMBIA1300-AtSGS3.

For RNA-silencing-suppression assays, all proteins were expressed from binary vectors as described in ref. 23. The C84S/C86S amino acid substitution

mutant of TYLCV V2 was produced as described in ref. 23. All PCRs were performed by using a high-fidelity Pfu DNA polymerase (Promega), and their products were verified by DNA sequencing.

***Arabidopsis* Growth Conditions and Transformation.** Seeds of *Arabidopsis thaliana L1-sgs3-1* EMS-mutant line (6) (a kind gift from H. Vaucheret, Institut National de la Recherche Agronomique Centre de Versailles, Versailles, France) were grown at 22°C in soil under a 16-h light/8-h dark regime.

For genetic complementation assays, *Agrobacterium*-mediated transformation of *L1-sgs3-1*, the *SGS3*-null mutant of *A. thaliana* ecotype Columbia, with *Agrobacterium tumefaciens* EHA105 carrying pCAMBIA1300-AtSGS3 or pCAMBIA1300-SlSGS3, was performed as described in ref. 40. The transformants were selected on growth medium supplemented with 20 mg/liter hygromycin.

Yeast Two-Hybrid Assay. A tomato cDNA library (38) was screened with pEG202-V2 as bait in *Saccharomyces cerevisiae* strain EGY48 as described in ref. 38, and positive clones were selected on a leucine-deficient medium, confirmed by β-gal assay (41), and isolated.

Agroinfiltration of Plant Tissues and Electroporation of Plant Protoplasts. Agroinfiltration was performed by using *A. tumefaciens* strain EHA105 (19). RNA-silencing suppression was assayed as described in ref. 23. To detect RNA-silencing suppression in whole leaves, we used *N. benthamiana* leaves, which express high levels of GFP, allowing its visualization at low magnification. For intracellular localization studies performed at higher magnification, we used young leaves of tomato, the native TYLCV host.

For protoplast transformation, leaf mesophyll protoplasts were isolated from *Nicotiana tabacum* L. cv. *Samsun* NN (42), and a mixture of 5 μg of plasmid DNA and 15 μg of calf thymus DNA was used for electroporation of 0.5 ml of protoplast solution (43). Transformed protoplasts were incubated in the dark for 46–48 h at 27°C before imaging.

Fluorescence Imaging. For confocal imaging, we used an Olympus IX 81 inverted laser scanning confocal microscope (Fluoview 500) equipped with an argon ion laser and a $\times$60 1.0 N.A. PlanApo water-immersion objective. CFP and YFP were excited at 458 and 515 nm and imaged by using BA480–495- and BA535–565-nm emission filters, respectively. For chlorophyll autofluorescence, a BA 660-nm IF emission filter was used. Transmitted light images were obtained by using Nomarski differential interference contrast.

Visual detection of GFP fluorescence in plant leaves was performed by using a Leica MZFLIII fluorescence stereomicroscope with a Leica DC200 camera. GFP was observed under a mercury lamp light by using a 450–490-nm excitation filter and a 500–550-nm emission filter. Photographic images were prepared by using Adobe Photoshop version 10.0 (Adobe Systems).

Detection of Protein–Protein Interactions by FRET Microscopy. The FRET procedure was performed by using the acceptor photobleaching method (30). CFP (donor) and YFP (acceptor) were excited at 70% and 3% laser power, respectively. All other conditions were as described for confocal imaging. The microscope was configured with a 458–515-nm dichroic mirror for dual excitation and a 515-nm beam splitter to help separate CFP and YFP fluorescence. Acceptor was bleached by scanning a region of interest (ROI) at 100% laser power, resulting in photobleaching of at least 90% of the original fluorescence. The pre- and postbleach images were collected, and ROI fluorescence intensity was measured by using Fluoview 500 software. Each measurement was conducted on a set of 10 different cells. The percentage of FRET efficiency (E_F) was calculated as $E_F = (I_{n+1} - I_n) \times 100/I_{n+1}$, where I_n and I_{n+1} are the CFP intensities at the time points between which the bleaching occurred (31).

PCR and RT-PCR. To detect the *SlSGS3* and *AtSGS3* transgenes, DNA was extracted from leaf tissue and assayed by PCR, which was designed to produce 786-bp- and 888-bp-specific fragments, respectively. Under these conditions, the endogenous *AtSGS3* gene yielded a 1,191-bp PCR product because of the presence of an intron.

For RT-PCR, 1 μg of RNA was extracted from frozen leaves with a TRI reagent (Sigma–Aldrich) according to the manufacturer's instructions. The RNA was reverse-transcribed by using a Reverse-iTTM 1st Strand Synthesis Kit (ABgene) and PCR-amplified to produce 992-bp, 921-bp, and 600-bp fragments specific for *SlSGS3*, *AtSGS3*, and *Actin*, respectively. PCR and RT-PCR products were resolved on a 1% agarose gel and detected by ethidium-bromide staining. The specificity of the amplification products was verified by DNA sequencing.

Quantification of GUS Expression. *Arabidopsis* mature rosette leaves were ground and assayed for GUS activity by using the fluorescent substrate 4-methylumbelliferyl β-D-galactoside as described in ref. 44. The enzymatic activity was expressed as nanomolar concentration of the fluorescent product 4-methylumbelliferone per microgram of total plant protein. All experiments were performed in triplicate, and the resulting data represent average values with indicated standard deviations.

ACKNOWLEDGMENTS. We thank Hervé Vaucheret (Institue National de la Recherche Agronomique, Versailles) for providing seeds of *A. thaliana* L1-sgs3-1 EMS mutant line. This work was supported by a U.S.–Israel Binational Research and Development grant (to V.C. and Y.G.). Y.G. is also supported by the Israel Science Foundation and the Israel Ministry of Science and Technology. V.C. is also supported by National Institutes of Health, National Science Foundation, and Binational Science Foundation grants. This paper is contribution 124/2007 from the Agricultural Research Organization, The Volcani Center, Bet Dagan, Israel.

1. Stram Y, Kuzntzova L (2006) *Virus Genes* 32:299–306.
2. Wang MB, Metzlaff M (2005) *Curr Opin Plant Biol* 8:216–222.
3. Vanitharani R, Chellappan P, Fauquet CM (2005) *Trends Plants Sci* 10:144–151.
4. Soosaar JL, Burch-Smith TM, Dinesh-Kumar SP (2005) *Nat Rev Microbiol* 3:789–798.
5. Vaucheret H (2006) *Genes Dev* 20:759–771.
6. Muangsan N, Béclin C, Vaucheret H, Robertson D (2004) *Plant J* 38:1004–1014.
7. Béclin C, Boutet S, Waterhouse P, Vaucheret H (2002) *Curr Biol* 12:684–688.
8. Mourrain P, Béclin C, Elmayan T, Feuerbach F, Godon C, Morel JB, Jouette D, Lacombe AM, Nikic S, Picault N, *et al.* (2000) *Cell* 101:533–542.
9. Zamore PD (2004) *Curr Biol* 14:R198–R200.
10. Chapman EJ, Prokhnevsky AI, Gopinath K, Dolja VV, Carrington JC (2004) *Genes Dev* 18:1179–1186.
11. Pooggin MM, Dreyfus M, Hohn T (2001) *Int Arch Biosci* 2001:1023–1026.
12. Vance V, Vaucheret H (2001) *Science* 292:2277–2280.
13. Baulcombe DC (2002) *Trends Microbiol* 10:306–308.
14. Bisaro DM (2006) *Virology* 344:158–168.
15. Voinnet O, Lederer C, Baulcombe DC (2000) *Cell* 103:157–167.
16. Silhavy D, Molnár A, Lucioli A, Szittya G, Hornyik C, Tavazza M, Burgyán J (2002) *EMBO J* 21:3070–3080.
17. Moissiard G, Voinnet O (2004) *Mol Plant Pathol* 5:71–82.
18. Reed JC, Kasschau KD, Prokhnevsky AI, Gopinath K, Pogue GP, Carrington JC, Dolja VV (2003) *Virology* 306:203–209.
19. Vargason JM, Szittya G, Burgyan J, Tanaka Hall TM (2003) *Cell* 115:799–811.
20. Ye K, Malinina L, Patel DJ (2003) *Nature* 426:874–878.
21. Zhang X, Yuan YR, Pei Y, Lin SS, Tuschl T, Patel DJ, Chua NH (2006) *Genes Dev* 20:3255–3268.
22. Bortolamiol D, Pazhouhandeh M, Marrocco K, Genschik P, Ziegler-Graff V (2007) *Curr Biol* 17:1615–1621.
23. Zrachya A, Glick E, Levy A, Arazi T, Citovsky V, Gafni Y (2007) *Virology* 358:159–165.
24. Fields S, Song O (1989) *Nature* 340:245–246.
25. Hollenberg SM, Sternglanz R, Cheng PF, Weintraub H (1995) *Mol Cell Biol* 15:3813–3822.
26. Gyuris J, Golemis E, Chertkov H, Brent R (1993) *Cell* 75:791–803.
27. Bateman A (2002) *BMC Bioinformatics* 3:21.
28. Hink MA, Bisselin T, Visser AJ (2002) *Plant Mol Biol* 50:871–883.
29. Jares-Erijman EA, Jovin TM (2003) *Nat Biotechnol* 21:1387–1395.
30. Kenworthy AK (2001) *Methods* 24:289–296.
31. Karpova TS, Baumann CT, He L, Wu X, Grammer A, Lipsky P, Hager GL, McNally JG (2003) *J Microsc* 209:56–70.
32. Elmayan T, Balzergue S, Beon F, Bourdon V, Daubremet J, Guenet Y, Mourrain P, Palauqui JC, Vernhettes S, Vialle T, *et al.* (1998) *Plant Cell* 10:1747–1758.
33. Vanitharani R, Chellappan P, Fauquet CM (2003) *Proc Natl Acad Sci USA* 100:9632–9636.
34. Lucioli A, Noris E, Brunetti A, Tavazza R, Ruzza V, Castillo AG, Bejarano ER, Accotto GP, Tavazza M (2003) *J Virol* 77:6785–6798.
35. Yoshikawa M, Peragine A, Park MY, Poethig RS (2005) *Genes Dev* 19:2164–2175.
36. Cohen S, Antignus Y (1994) *Adv Disease Vector Res* 10:259–288.
37. Xu L, Yang L, Pi L, Liu Q, Ling Q, Wang H, Poethig RS, Huang H (2006) *Plant Cell Physiol* 47:853–863.
38. Zhou J, Loh YT, Bressan RA, Martin GB (1995) *Cell* 83:925–935.
39. Tzfira T, Tian GW, Lacroix B, Vyas S, Li J, Leitner-Dagan Y, Krichevsky A, Taylor T, Vainstein A, Citovsky V (2005) *Plant Mol Biol* 57:503–516.
40. Clough SJ, Bent AF (1998) *Plant J* 16:735–743.
41. Durfee T, Becherer K, Chen PL, Yeh SH, Yang Y, Kilburn AE, Lee WH, Elledge SJ (1993) *Genes Dev* 7:555–569.
42. Draper J, Scott R, Armitage P, Walden R (1988) *Plant Genetic Transformation and Gene Expression: A Laboratory Manual* (Blackwell Scientific, Oxford).
43. Fromm M, Taylor LP, Walbot V (1985) *Proc Natl Acad Sci USA* 82:5824–5828.
44. Nam J, Mysore KS, Zheng C, Knue MK, Matthysse AG, Gelvin SB (1999) *Mol Gen Genet* 261:429–438.